

SCALE INHIBITOR ADSORPTION STUDIES IN ROCK SANDSTONE TYPE

C. B. Veloso¹, T. T. G. Watanabe¹, A. N. A. Silva², J. F. B. C. Paes¹, F. M. T. Luna¹, C. L. Cavalcante Jr¹

1- Departamento de Engenharia Química – Universidade Federal do Ceará
Campus do Pici S/nº, Bloco 709 – CEP: 60.455-900 – Fortaleza-CE – Brasil
Telefone: (85) 3366-9611 – Fax: (00) 3366-9598 – Email: celio@gpsa.ufc.br

2- Departamento de Engenharia Mecânica e de Produção – Universidade Federal do Ceará
Campus do Pici S/nº, Bloco 709 – CEP: 60.455-760 – Fortaleza-CE – Brasil
Telefone: (85) 3366-9632 – Fax: (85) 3366-9636 – Email: alvaro_neuton@hotmail.com

ABSTRACT: In oil recovery in petroleum reservoir, the most used process is seawater injection. However, this method causes scale formation which damage the production structures. These deposits can be derived from the incompatibility between the seawater and formation water and can be formed from pressure drop. To prevent the formation of deposits applies squeeze method which the scale inhibitors are injected into the well. Therefore, this study aimed to analyze the interaction between the commercial scale inhibitor and the sandstone rock, evaluating the influence of temperature and inhibitor concentration by test in fixed bed. It was observed through temperature increase a rise in the adsorption capacity from 3.03 to 6.17 mg g⁻¹, which can be explained by the density of electrostatic charges on the rock surface. This system was modeled, and it resulted in a good correlation with the proposed model.

KEYWORDS: adsorption, squeeze, scale inhibitor, sandstone rock.

1. INTRODUCTION

There are some reservoirs which do not have pressure enough to lift the oil at surface. It needs technologies to promote this displacement, such as gas lift, pumping and water flooding (Punternvold e Austad, 2008; Alemi et al., 2011). The most used technic is water flooding that, in offshore wells, the seawater is selected to be injected in the well (Sorbie e Mackay, 2000; Bader, 2006; Bader, 2007; Binmerdhah et al., 2010).

The seawater injected is rich in sulfate ions (SO₄²⁻) and formation water has barium (Ba²⁺), magnesium (Mg²⁺), strontium (Sr²⁺), calcium (Ca²⁺) and others cations in high concentration, forming insoluble sulfate salts when these waters are mixed (Yuan et al., 1994; Bedrikovetsky et al., 2009; Senthilmurugan et al., 2011). Beyond sulfates, carbonates are found and this one is formed by pressure drop in the wellbore (Zhang e Dawe, 1998; Zhang et al., 2001).

These salts can deposit on the production lines and near wellbore formation. This deposition

blocks the flow, promotes production loss and can deactivate all the production structure (Andrei e Gagliardi, 2004; Martinod et al., 2008; Kumar et al., 2010).

The technology used to avoid the scale formation is squeeze treatment, which scale inhibitor is injected in the wellbore. It may be adsorbed or precipitated on the rock surface (Rabaioli e Lockhart, 1996; Andrei e Gagliardi, 2004). The adsorption is the retention mechanism more convenient than precipitation one in squeeze process because the material deposition or precipitation is minimized, reducing others problems while the treatment is done (Tantayakom et al., 2005).

In laboratory, coreflood tests simulate the wellbore conditions to study the interaction rock-inhibitor and evaluate rock damage after squeeze treatment (Ochi e Vernoux, 1998; Rocha et al., 2004). In this test the rock is confined and inhibitor flows through it.

The aim of this paper is analyze the behavior of adsorption process of scale inhibitor on the rock



surface. The inhibitor concentration and temperature influence also will be evaluated.

The adsorption tests were carried out using aminomethylene phosphonic acid as scale inhibitor and a fragmented sandstone rock. Mathematical modeling was used to simulate the process and to determinate mass transfer parameters.

2. MATERIALS AND METHODS

2.1. Materials

Adsorption tests were carried out using the sandstone rock (about 90% SiO₂) provided by CENPES/Petrobras. This rock was fragmented in particles with 605 μm medium diameter. The commercial inhibitor used in the tests has about 17% of aminomethylene phosphonic acid as the active phase.

2.2. Methods

The rock was characterized by N₂ isotherms at 77K to determinate surface area and total pore volume, measured in Autosorb (Quantachrome, USA). The surface area was calculated using BET methodology. The total pore volume was obtained from the N₂ volume adsorbed at a relative pressure of 0.994. The density was determined by experiments with Helium in a magnetic suspension balance Rubotherm (Bochum, Alemanha). With this method was determined solids volume and particle porosity (Equation 1).

$$\varepsilon_p = \frac{V_p}{V_p + V_s} \quad (1)$$

which ε_p is the particle porosity, V_s is solids volume and V_p is total pore volume.

Experimental apparatus for adsorption tests consists of a steel column which was coupled to pump system ProStar 210 Varian (90% accuracy) and oven to control the flow and temperature.

The operating flow was 0.1 mL min⁻¹ and the scale inhibitor concentrations injected in the column were 1 to 10 mg mL⁻¹. The tests were carried out at temperatures 323.15 and 353.15 K. The column effluent was analyzed by ICP-OES. The compound used to determinate the inhibitor concentration was the phosphorus.

The bed porosity (ε) was determined by Equation 2.

$$\varepsilon = 1 - \left(\frac{M_L}{V_L \rho_s} \right) \quad (2)$$

which M_L is the adsorbent mass (g), V_L packed bed volume (mL), determined by the dimensions of the column and ρ_s is the rock density.

To determine the adsorption capacity (q^*) carried out a mass balance in the column (Equation 3), which the flow was considered distributed equally in transversal section.

$$q^* = \frac{C_0}{M_L} \left[Q \int_0^1 \left(1 - \frac{C}{C_0} \right) dt - V_L \varepsilon \right] \quad (3)$$

which q^* is adsorption capacity (mg g⁻¹), C_0 initial concentration (mg L⁻¹), C final concentration (mg L⁻¹), Q flow rate (mL min⁻¹).

Isotherms data experiments were treated by Langmuir equation (Equation 4).

$$\frac{q^*}{q_m} = \frac{b C_{eq}}{1 + b C_{eq}} \quad (4)$$

which q_m is adsorption maximum capacity (mg g⁻¹), b is affinity between adsorbate and adsorbent (mL mg⁻¹) and C_{eq} concentration in equilibrium in the liquid phase (mg mL⁻¹).

The experiments values were compared with calculated values by medium percentual deviation (%D) expressed by Equation 5 (Berber-Mendoza et al., 2006).

$$\%D = \sum \frac{|q_e - q_c|}{q_e} \times \frac{100}{N} \quad (5)$$

which q_e and q_c are the experimental and calculated adsorption capacity and N is the number of experiments.

Linear Drive Force model (LDF) was used to predict the breakthrough curves and validate the experimental data (Equations 6 to 11). For all modeling was used Langmuir equation to represent the equilibrium of the system (Ruthven, 1984; Cooney, 1999; Dantas et al., 2011).

$$\varepsilon \frac{\partial C}{\partial t} + \rho_s (1 - \varepsilon) \frac{\partial \bar{q}}{\partial t} + v_s \frac{\partial C}{\partial z} = \varepsilon D_{ax} \frac{\partial^2 C}{\partial z^2} \quad (6)$$

$$\frac{\partial \bar{q}}{\partial t} = K_L (q^* - \bar{q}) \quad (7)$$

Initial conditions:

$$t = 0 \quad C(z, 0) = 0 \quad (8)$$

$$t = 0 \quad \bar{q}(z, 0) = 0 \quad (9)$$

Boundary conditions:

$$\frac{\partial C(0, t)}{\partial z} = \frac{v_s}{\varepsilon D_{ax}} [C(0, t) - C_0] \quad (10)$$

$$\frac{\partial C(L, t)}{\partial z} = 0 \quad (11)$$

which C is adsorbate concentration in fluid phase (mg mL^{-1}), \bar{q} adsorbate average capacity in the solid phase (mg g^{-1}), D_{ax} axial dispersion coefficient ($\text{cm}^2 \text{min}^{-1}$), v_s superficial velocity (cm min^{-1}) and K_L coefficient mass transfer effective (min^{-1}).

The axial dispersion coefficient was estimated from the correlation using Peclet and Reynolds numbers (Butt, 1980) as shown in Equation 12.

$$\varepsilon \frac{D_{ax}}{v_s d_p} = 0.2 + 0.011 \text{Re}^{0.48} \quad (12)$$

which d_p is particle diameter (cm).

The coefficient mass transfer effective was estimated using heterocedastic estimation method of the computational package gPROMS®.

3. RESULTS AND DISCUSSION

The profile of N_2 adsorption and desorption isotherms (Figure 1) shown the sandstone rock used in this work has low porosity, because the isotherm is of type III, according BDDT classification (Thomas e Crittenden, 1998).

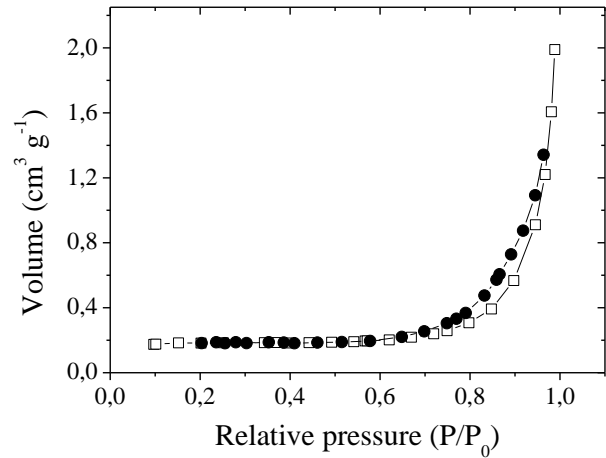


Figure 1. N_2 (\square) adsorption and (\bullet) desorption isotherms at 77K of sandstone rock.

In Table 1 is shown the values obtained to the particle surface area specific (S_{BET}), pore volume (V_p), rock density (ρ_s), solid volume (V_s) and particle porosity (ε_p).

Table 1. Textural properties of the rock particles.

Properties	Results
S_{BET} ($\text{m}^2 \text{g}^{-1}$)	0.51
V_p ($\text{cm}^3 \text{g}^{-1}$)	3.08×10^{-3}
ρ_s (g cm^{-3})	2.66
V_s (cm^3)	0.45
ε_p	0.0068

It is noted that the material has low porosity, confirming the isotherm profile. Furthermore, the low porosity results in the low pore volume, suggesting the adsorption process happens basically in the solid particle surface.

The column was packed with fragmented rock uniformly and in Table 2 is shown the bed characteristics.

Table 2. Bed characteristics.

Properties	Results
ε	0.57
D_{ax} ($\text{cm}^2 \text{min}^{-1}$)	0.178



With the data obtained by testing on fixed bed were plotted the breakthrough curves for each concentration used in each temperature. With the mass balance, the adsorption isotherms for the inhibitor were plotted as illustrated in Figure 2. The fitted curves have their adsorption maximum capacities estimated for each system, following Langmuir.

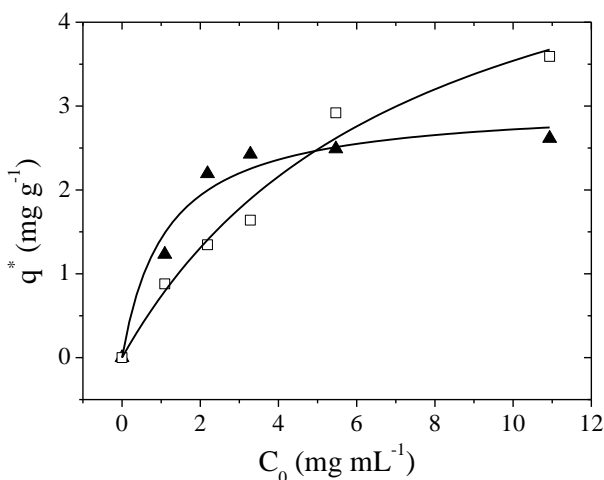


Figure 2. Adsorption isotherms of scale inhibitor solution at (\blacktriangle) 323.15K and (\square) 353.15K temperatures. Isotherms fit by (\rightarrow) Langmuir.

The fitted curves have their adsorption maximum capacities estimated for each system, following Langmuir equation. The parameters are reported in Table 3.

Table 3. Parameters of Langmuir equation.

Parameters	323.15K	353.15K
q_m (mg g^{-1})	3.03 ± 0.24	6.17 ± 0.971
b (mL mg^{-1})	0.88 ± 0.28	0.135 ± 0.039
R^2	0.97	0.98
%D	7.11	7.08

It is observed there was an increase in the adsorption capacity of 3.03 to 6.17 mg g^{-1} when the temperature rises. In physics adsorption this fact is not common, so may be occurred an ionic exchange probably because occurred electrostatic changes in the rock surface, intensifying

interactions between the inhibitor and the rock, which increases the amount of adsorbed inhibitor.

This phenomenon of electrostatic surface modification of silica materials observed by Waseem et al. (2011), who did the adsorption of Cd (II) on SiO_2 . It was observed the adsorption of metal increased from 0.033 to $0.043 \text{ mmol g}^{-1}$ when the temperature changes from 288.15 to 318.15K in a finite bath experiments and the authors justification was the material surface electrostatic alteration.

In Figure 3 to Figure 5 is shown all the breakthrough curves simulated using gPROMS at 323.15 and 353.15K to some concentrations.

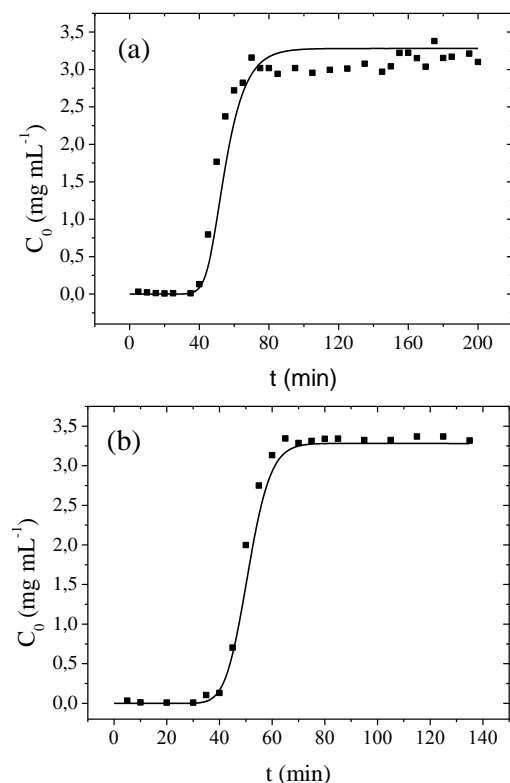


Figure 3. Experimental and simulated breakthrough curves at 3.0 mg mL^{-1} at (a) 323.15 K and (b) 353.15K.

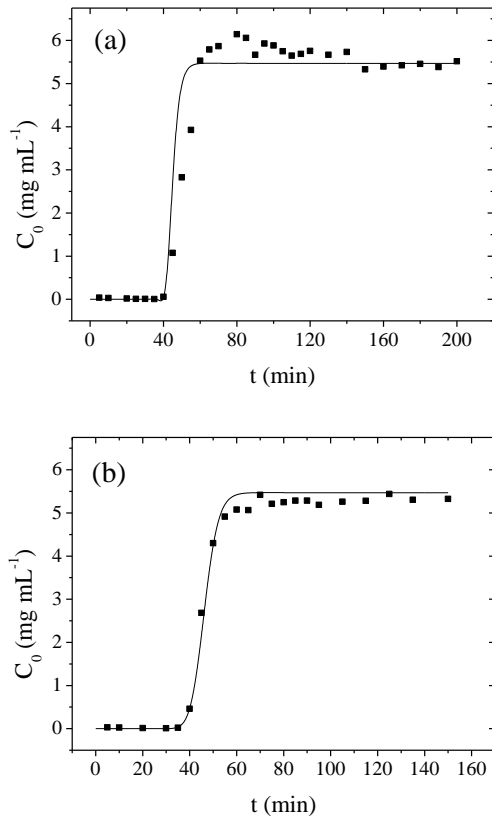


Figure 4. Experimental and simulated breakthrough curves at 5.0 mg mL⁻¹ at (a) 323.15 K and (b) 353.15K.

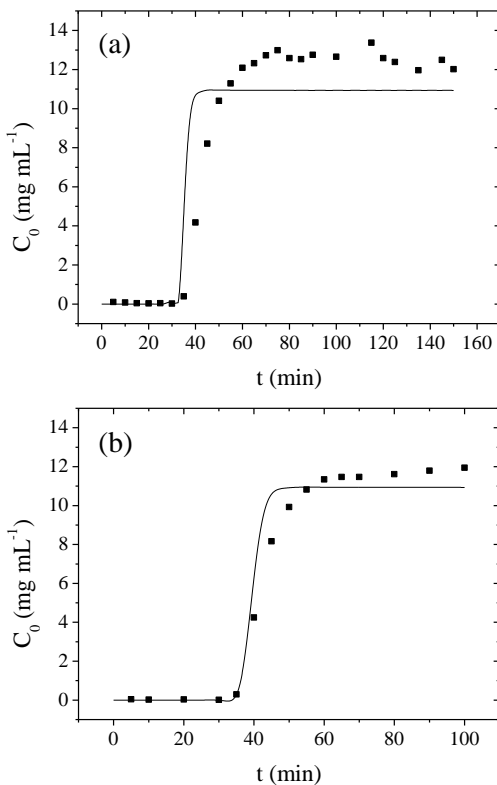


Figure 5. Experimental and simulated breakthrough curves at 10.0 mg mL⁻¹ at (a) 323.15 K and (b) 353.15K.

There was good agreement between the experimental curves and the curves obtained from the simulations. To confirm that the models employed generated good predictions of concentration profiles at the outlet of the column was employed analysis of variance (ANOVA) with a significance level of 0.05 to detect differences between the experimental data and the data obtained by simulations. All parameter values p were higher than 0.70, attesting to the reliability of the simulations.

The mass transfer parameters K_L estimated by LDF model applied in this paper are shown in Table 4.

Table 4. Mass transfer parameters estimated.

T (K)	C_0 (mg mL ⁻¹)	K_L (min ⁻¹)
323.15	3.281	0.150
	5.468	0.530
	10.935	0.968
353.15	3.281	0.765
	5.468	0.992
	10.935	1.818

Low values of the K_L represent the high resistance of the inhibitor flow to active sites. The rock has a low porosity, so the flow resistance is restricted to the fluid film around the particle.

To solve this problem could be increased the flow rate, because the system will be more turbulent and it gets mass transfer easier to cross through the boundary layer around the particle.

In squeeze operations, which after the inhibitor injection the production is stopped, the inhibitor probably will be transferred by molecular diffusion and it will break the fluid film. Therefore, when the well is opened, the inhibitor may not be adsorbed on the rock then it could not avoid the scale formation. In this case, to solve this



resistance the best form will be the shut in time to increase the efficiency of the treatment.

4. CONCLUSION

In this paper was studied adsorption of scale inhibitor on the sandstone rock. It was evaluated the temperature, inhibitor concentration and pH influence in the adsorption in fixed bed tests.

The rock textural characteristics, determined by N₂ isotherms, showed low values of surface area, pore volume and porosity. These characteristics contributed to the small quantities of inhibitor adsorbed in the solid, 3.03 and 6.17 mg g⁻¹, following the Langmuir equation. Langmuir equation was used to fit experimental points of isotherm and gave good results (R² > 0.97) which the deviation did not exceed 7%.

The mathematical model proposed to simulate the experimental data was satisfactory in fitting the data and estimating of the coefficient mass transfer effective. Based on the results obtained in the estimation of K_L was confirmed the scale inhibitor is adsorbed around the rock surface because the particle showed low diffusivity in the few pores in the adsorbent particle.

5. REFERENCES

ALEMI, M.; JALALIFAR, H.; KAMALI, G. R.; KALBASI, M.; PEDEC RESEARCH & DEVELOPMENT. A mathematical estimation for artificial lift systems selection based on ELECTRE model. *J. Pet. Sci. Engineering*, v. 78, p. 193-200, 2011.

ANDREI, M.; GAGLIARDI, F. Redissolution studies in bulk and in coreflood for PPCA scales inhibitor. *J. Pet. Sci. Engineering*, v. 43, p. 35-55, 2004.

BADER, M.S.H. Sulfate scale problems in oil fields water injection operations. *Desalination*, v. 201, p. 100-105, 2006.

BADER, M.S.H. Sulfate removal technologies for oil fields seawater injection operations. *J. Pet. Sci. Engineering*, v. 55, p. 93-110, 2007.

BEDRIKOVETSKY, P.; SILVA, R. M. P.; DAHER, J. S.; GOMES, J. A. T.; AMORIM, V. C. Well-data-based prediction of productivity decline

due to sulphate scaling. *J. Pet. Sci. Engineering*, v. 68, p. 60-70, 2009.

BERBER-MENDOZA, M. S.; LEYVA-RAMOS, R.; ALONSO-DAVILA, P.; FUENTES-RUBIO, L.; GUERRERO-CORONADO, R.M. Comparison of isotherms for the ion exchange of Pb(II) from aqueous solution onto homoionic clinoptilolite. *J. Colloid Interface Sci.*, v. 301, p. 40-45, 2006.

BINMERDHAH, A. B.; YASSIN, A. A.; MUHEREI, M. A. Laboratory and prediction of barium sulfate scaling at high-barium formation water. *J. Pet. Sci. Engineering*, v. 70, p. 79-88, 2010.

BUTT, J.B.: *Reaction Kinetics and Reactor Design*. Englewood Cliffs: Prentice Hall, 1980.

COONEY, D. O. *Adsorption Design for Wastewater Treatment*, USA: Lewis Publishers, 1999.

DANTAS, T. L. P.; LUNA, F. M. T.; SILVA JR., I. J.; AZEVEDO, D. C. S.; GRANDE, C. A.; RODRIGUES, A. E.; MOREIRA, R. F. P. M. Carbon dioxide-nitrogen separation through adsorption on activated carbon in a fixed bed. *Chem. Eng. J.*, v. 169, p. 11-19, 2011.

KUMAR, T.; VISHWANATHAM, S.; KUNDU, S. S. A laboratory study on pteroyl-L-glutamic acid as a scale prevention inhibitor of calcium carbonate in aqueous solution of synthetic produced water. *J. Pet. Sci. Engineering*, v. 71 p. 1-7, 2010.

MARTINOD, A.; EUVRARD, M.; FOISSY, A.; NEVILLE, A. Progressing the understanding of chemical inhibition of mineral scale by green inhibitors. *Desalination*, v. 220, p. 345-352, 2008.

OCHI, J.; VERNOUX, J-F. Permeability decrease in sandstone reservoirs by fluid injection – Hydrodynamic and chemical effects. *J. Hydrol.*, v. 208, p. 237-248, 1998.

PUNTERVOLD, T.; AUSTAD, T. Injection of seawater and mixtures with produced water into North Sea chalk formation: Impact of fluid-rock interactions on wettability and scale formation. *J. Pet. Sci. Engineering*, v. 63, n. 1-4, p. 23-33, 2008.



RABAIOLI, M. R.; LOCKHART, T. P. Solubility and phase behavior of polyacrylate scale inhibitors. *J. Pet. Sci. Engineering*, v. 15, p. 115-126, 1996.

ROCHA, A. A.; MIEKELEY, N.; BEZERRA, M. C. M.; KÜCHLER, I. L. An automated system for preconcentration/matrix-removal followed by ICP-MS determination of organic phosphorus in oil production water. *Microchem. J.*, v. 78, p. 65-70, 2004.

RUTHVEN, D.M. *Principles of Adsorption and Adsorption Processes*. New York: John Wiley & Sons, 1984.

SENTHILMURUGAN, B.; GHOSH, B.; SANKER, S. High performance maleic acid based oil well scale inhibitors - Development and comparative evaluation. *J. Ind. Eng. Chem.*, v. 17, p. 415-420, 2011.

SORBIE, K. S.; MACKAY, E. J. Mixing of injected, connate and aquifer brines in waterflooding and its relevance to oilfield scaling. *J. Pet. Sci. Engineering*, v. 27, p. 85-106, 2000.

TANTAYAKOM, V.; FOGLER, H. S.; CHAROENSIRITHAVORN, P.; CHAVADEJ, S. Kinetic study of scale inhibitor precipitation in squeeze treatment. *Cryst. Growth Des.*, v. 5, n°1, p. 329-335, 2005.

THOMAS, W. J.; CRITTENDEN, B. *Adsorption Technology and Design*. Elsevier Science & Technology Books, 1998.

YUAN, M.; TODD, A. C.; SORBIE, K. S. Sulphate scale precipitation arising from seawater injection: a prediction study. *Mar. Petrol. Geol.*, v. 11, n° 1, p. 24-30, 1994.

WASEEM, M.; MUSTAFA, S.; NAEEM, A.; SHAH, K.H.; SHAH, I. Mechanism of Cd (II) sorption on silica synthesized by sol-gel method. *Chem. Eng. J.*, v. 169, p. 78-83, 2011.

ZHANG, Y.; DAWE, R. The kinetics of calcite precipitation from a high salinity water. *Appl. Geochem.*, v. 13, p. 177-184, 1998.

ZHANG, Y.; SHAW, H.; FARQUHAR, R.; DAWE, R. The kinetics of carbonate scaling —

application for the prediction. *J. Pet. Sci. Engineering*, v. 29, p. 85-95, 2001.

6. ACKNOWLEDGMENTS

The financial support of Petrobras and Capes. The textural characterizations of Universidad de San Luis (Argentina).